Available online at www.sciencedirect.com
SCIENCE DIRECT®
Journal of Photochemistry and Photobiology A: Chemistry 158 (2003) 125–130
Journal of Photochemistry and Photobiology A:Chemistry
www.elsevier.com/locate/jphotochem

Dye-sensitized photoelectrochemical and solid-state solar cells: charge separation, transport and recombination mechanisms

K. Tennakone*, P.V.V. Jayaweera, P.K.M. Bandaranayake

Institute of Fundamental Studies, Hantana Road, Kandy, Sri Lanka

Received 20 March 2002; received in revised form 18 June 2002; accepted 1 July 2002

Abstract

Experiments on dye-sensitized (DS) photoelectrochemical cells made from SnO_2, ZnO and comparison with similar cells based on TiO_2 gives much insight into the nature of charge separation, transport and recombinations. It is shown that the trap mediated recombinations are sensitive to the effective electron mass and therefore explains difference between the cells made from TiO_2 and SnO_2 or ZnO. Considering the trap mediated electron leakage from nanocrystallites, a theoretical model is constructed to explain quantitatively the effect of trapping on static and transient behavior of the cells. The model clearly demonstrate that trapping seriously affects the performance of the cell, when the electron leakage from traps is significant. The predictions of the model are compared with experimental data on transient measurements. The paper will also comment on the problem of recombinations in DS solid-state cells.

Keywords: Dye-sensitization; Photoelectrochemical cells; Charge recombination; Nanoparticles; Nanocrystalline films; Electron trapping; Tin(IV) oxide

1. Introduction

The optimized dye-sensitized (DS) solar cells made from nanocrystalline films of TiO_2 [1] sensitized with ruthenium bipyridyl dyes have efficiencies (η) ~10% at one sun conditions [2]. The reported values of the short-circuit photocurrent (I_{sc}) and the open-circuit voltage (V_{oc}) under same conditions are of the order 20 mA cm^{-2} and 800 mV, respectively. The photocurrent seems to be close to the value expected from consideration of photon to photocurrent conversion efficiency (IPCE) in relation to the solar spectrum. However, the V_{oc} is below the theoretical upper limit, which is the difference between the energy positions of the redox-couple (I^-/I_3^-) and the conduction band edge of TiO_2. Recombinations reduce the V_{oc} by making it difficult for the quasi-Fermi level (QFL) to rise up to the conduction band edge of TiO_2. It is remarkable that the Gratzel's cell which exposes an interface (the potential site of recombinations) of nearly 1000 times the geometrical area could generate a V_{oc} as high as 800 mV indicating that there is an inherent mechanism of controlling recombination in this device.

Electrons injected to the conduction band in a DS device could undergo four distinct types of recombinations, i.e. (1) geminate recombination with the dye cations D^+; (2) non-geminate e^-, D^+ recombinations; (3) reaction with an acceptor (e.g. I_3^-) in the electrolyte at the semiconductor/electrolyte interface; (4) reaction with acceptors in the electrolyte at the exposed conducting glass/electrolyte interface. Of these the rate of (1) is believed to be very small because of the fastness [3–5] of electron in injection and slowness [6–8] of the back reaction. As positive charge on D^+ is scavenged quite rapidly, the rate of (2) could become important only at extremely high intensities. The rate of (4) is also determined to be small and therefore (3) becomes the most important recombination mode. This is to be expected as the semiconductor/electrolyte interface spans an area nearly three orders of magnitude the geometrical projection of light absorbing area (owing to the large roughness factor of the film) and electrons become susceptible to this mode of recombinations through out their path to the back contact. Recombinations also have an effect on the photocurrent. The diffusion length of electrons in the nanocrystalline film can be expressed as $(D\tau)^{1/2}$, where D is the diffusion coefficient of electrons in the nanocrystalline matrix and $\tau^{-1} = \tau_1^{-1} + \tau_2^{-1} + \tau_3^{-1}$ (τ_1, τ_2, τ_3 being the recombination times of the processes (1), (2) and (3)). Thus if $(D\tau)^{1/2}$ is greater than the mean free path of light in the film, a good portion of electrons get lost in recombinations thereby decreasing the I_{sc}. Here again the most significant loss mechanism is the process (3).

* Corresponding author. Tel.: +94-8-232001/2; fax: +94-8-232131.
E-mail address: tenna@ifs.ac.lk (K. Tennakone).

1010-6030/03/$ – see front matter © 2003 Elsevier Science B.V. All rights reserved.
doi:10.1016/S1010-6030(03)00026-1

The mode of electron transport along nanocrystallites is not fully understood and many models have been studied [9–16]. Experimentally determined diffusion coefficients represents the gross effect of individual events occurring in the nanocrystalline path (i.e. trapping, detrapping and transit across the neck regions of the crystallite contacts) as well as the influence of the electrolyte. Electrons injected to a semiconductor in dye-sensitization, relaxes to the bottom of the conduction band and would also enter into shallow traps from which they are re-emitted back to the conduction band. Transport could be via conduction band states or trap-to-trap hopping. As the diffusion coefficients associated with trap-to-trap hopping are smaller than those corresponding to dispersive transport in the conduction band, in the discussion that follows, we will ignore the trap-to-trap transport. The recombinations of electrons with acceptors in the electrolyte could also be via conduction band or trap states. We have obtained convincing evidence that the recombinations of the type (3) involves, predominantly the electrons trapped in shallow levels [17–19]. Experimentation on dye-sensitization of nanocrystalline films of SnO_2 [17–20], ZnO [20,21], CdS and composites films enabled us to gain much understanding of the nature of recombinations and explain why TiO_2 behaves differently from SnO_2 and ZnO which have similar band positions and adsorbs ruthenium bipyridyl dyes to an extent comparable to TiO_2. The greatest difficulty in describing quantitatively the transport and recombination in DS cells, originates from the dependence of the rates of these processes on the electron occupation. Thus the transport equations become highly nonlinear making mathematical analysis exceedingly complex.

Results obtained from somewhat simplified models and comparison with experimental data will be presented in this paper.

2. Experimental

Most experiments are conducted with nanocrystalline films of SnO_2 (crystallite size 5–10 nm) or Sb-doped SnO_2 (Sb-SnO_2) films of same crystallite size. Films are prepared by spraying a colloidal solution of SnO_2 containing acetic acid onto conducting tin oxide glass heated to ∼150 °C and sintering at 450 °C in air for 30 min. SnO_2 and Sb-SnO_2 coated with an outer shells of MgO or ZnO (denoted by [SnO_2]MgO, [SnO_2]ZnO, [Sb-SnO_2]MgO, [Sb-SnO_2]ZnO, respectively) were prepared by adding a calculated amount of MgO or ZnO to the SnO_2 dispersion and sufficient acetic acid to dissolve the oxide [17,18]. Pyrolysis of the acetates (Mg or Zn) covers SnO_2 crystallites with an ultra-thin outer shell of MgO or ZnO. An alternative method used was to boil the SnO_2 coated films in alcoholic solution (99% ethanol) of zinc or magnesium acetates (∼10^{-3} M) and sinter at 450 °C for 10 min. Here the oxides of Mg or Zn gets deposited on SnO_2 by hydrolysis of the acetates. This pretreatment process was an attempt to cover only the outer surface of the crystallites with the shell material and avoid interposing of the crystallite contacts with MgO or ZnO. CdS colloidal particles were prepared by bubbling H_2S into a vigorously agitated solution of cadmium acetate in propan-1-ol. CdS particles separated by centrifugation are washed with ethanol and ground with carbowax (∼0.5% by the estimated weight of CdS) and sintered at 450 °C. CdS films were also electrodeposited by a literature method [22] using a solution cadmium chloride containing sulfur. The crystallites in CdS films were coated with MgO by treatment with magnesium acetate as in the case of SnO_2. Particle sizes and thickness of the films were measured with a SEM. Direct measurement of the thickness of outer shells of MgO and ZnO on SnO_2 was not possible by SEM or TEM and the shell thickness was estimated by determination of the amount oxide (MgO or SnO_2) per unit area of the film by chemical analysis and from a knowledge of the roughness factor of the film (i.e. shell thickness = weight of oxides per unit area/roughness factor × density of the oxide). The dye used in all experiments was *N*-bis(2,2′-bipyridyl-4,4′-dicarboxylic acid) Ru(II) coated by warming the plates deposited with various films in an alcoholic solution (0.5×10^{-3} M ethanol). Amount of dye adsorbed into the films were estimated by desorbing the dye into an alkaline alcoholic solution (5×10^{-3} M NaOH in 95% ethanol) and spectrophotometric estimation of the dye content in the extract. Roughness factor of the films were estimated assuming that each dye molecule covers an area of 1 nm^2 and compared with the values obtained from consideration of the particle sizes.

Photoelectrochemical cells were formed by clamping the dye coated film against a lightly platinized conducting tin oxide glass counter electrode and filling the capillary space with the electrolyte (0.6 M dimethylpropyl imidazolium iodide + 0.1 M LiI + 0.05 M I_2 + 0.5 M *t*-butyl pyridine in methoxy-acetonitrile). *I–V* characteristics (i.e. plot of current versus voltage) of the cells were measured using a Keithly Source Meter 2420 3A with a 2000 W m^{-2} Solar Simulator (Arctron). Simulator lamp intensity was calibrated with an Eko Pyranometer. Photocurrent and photovoltage transients were recorded with a homemade set up, where a collimated white light beam from a halogen lamp is interposed by a fast (<1 ms) mechanical shutter and the response was recorded on an oscilloscope.

3. Results and discussion

Following distinct differences were seen in DS cells made SnO_2 films when compared to similar cells made from TiO_2 films. (1) Despite attempts to optimize the performance, DS SnO_2 cells gave very low efficiencies (∼1%), poor fill factors (∼40%), open-circuit voltage (∼330 mV) which is much lower than the upper limit (∼600 mV) and a short-circuit photocurrent ∼12 mA cm^{-2}. However, in the cells made from the [SnO_2]MgO films (MgO shell thickness

Table 1
Photovoltaic parameters of cells made from films listed in the column 1

Film	I_{sc} (mA cm^{-2})	V_{oc} (mV)	FF (%)	η (%)
SnO_2	12.5	330	31	1.3
[SnO_2]MgO	15.4	654	65	6.0
[Sb-SnO_2]	$<10^{-2}$	$\sim10^{-1}$	–	$<10^{-4}$
[Sb-SnO_2]MgO	7.3	473	–	1.8
CdS	0.1	400	<10	0.05
[CdS]MgO	6.0	800	44	2.1

∼0.8 nm) a dramatic enhancement of the efficiency (∼6%), fill factor (∼65%), open-circuit voltage (∼700 mV) and the short-circuit photocurrent (∼15 mA cm^{-2}) were observed. The same effect was noticeable in DS cells made from [SnO_2]ZnO and [CdS]MgO films (Table 1). A distinct difference in SnO_2 and Sb-SnO_2 DS cells were also noticed. DS Sb-SnO_2 cells showed only a marginal photoresponse ($I_{sc} < 10^{-2}$ mA cm^{-2}, $V_{oc} < 10^{-1}$ mV). However, on deposition of ultra-thin outer shells (MgO or ZnO) on SnO_2 crystallites before coating the dye, a good photovoltaic response became noticeable once again ($I_{sc} \sim 7$ mA cm^{-2}, $V_{oc} \sim 475$ mA cm^{-2}, Table 1). We were able to demonstrate that the dye is anchored to the outer surface of the shell.

Photocurrent and photovoltage transients DS cells made from SnO_2, [SnO_2]MgO and [Sb-SnO_2]MgO presented in Figs. 1–3, have following general features. The rise and decay of the transient response (i.e. switch-on and switch-off) become faster in the presence of the MgO shell on SnO_2 in the film. These responses are significantly slower in DS [Sb-SnO_2]MgO compared to DS [SnO_2]MgO or [Sb-SnO_2]MgO. Furthermore an intensity dependence could be seen, i.e. transient responses become faster at higher light intensities. Again we noticed that the transient signals in DS [SnO_2]MgO are more sharper compared DS TiO_2 under same conditions. In the following section we attempt to explain the above observations quantitatively.

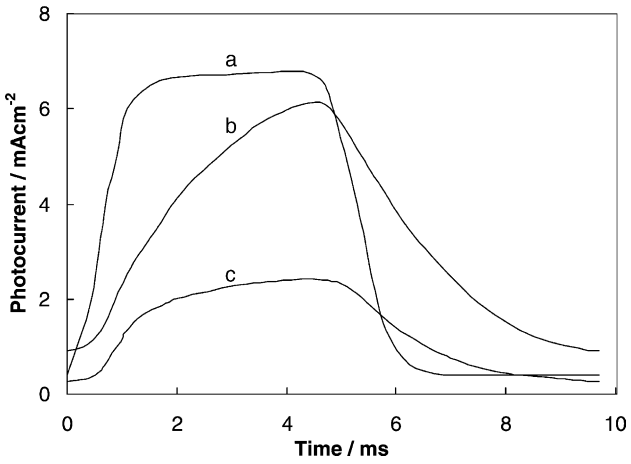

Fig. 2. Growth of short-circuit current (photocurrent, light-on transient) in DS PECs made from (a) [SnO_2]MgO, (b) TiO_2 and (c) SnO_2 films.

We have explained earlier that the distinction between TiO_2 and SnO_2 with respect to DS solar cell performance depends on the difference in the effective electron masses (m^*) in the two cases. Since the conduction band of TiO_2 originates from d-orbitals, the effective electron mass takes a high value (∼10 and 50m_e according to some reports). Whereas the s-orbital conduction band of SnO_2 gives rise to a smaller electron effective mass (∼0.1m_e). Electrons injected to the conduction band via dye sensitization, relaxes and transits up and down between thermally excitable shallow traps and states just above the conduction band edge (CBE). An electron trapped in a shallow level E below the CBE can be described by a wave function of the form [23]

$$\Psi(r) = A \exp\left(-\frac{r}{a}\right), \quad a = \frac{h}{2\pi(2m^*E)^{1/2}} \tag{1}$$

where h is the Planck's constant. When the crystallite radius r_c becomes comparable to a, the wave function strongly

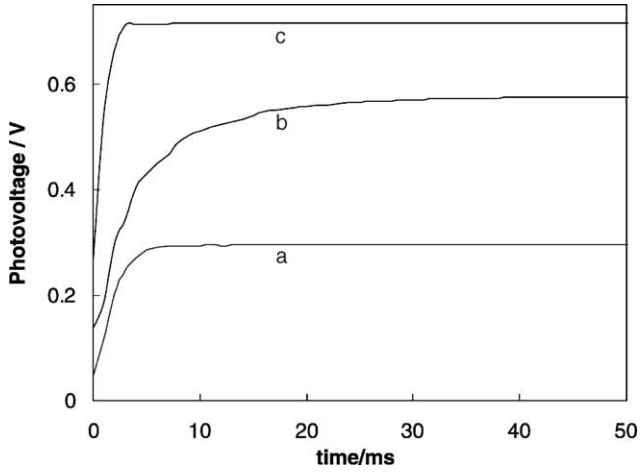

Fig. 1. Growth of open-circuit voltage (photovoltage, light-on transient) in DS PECs made from (a) SnO_2, (b) [SnO_2]MgO and (c) [Sb-SnO_2]MgO films.

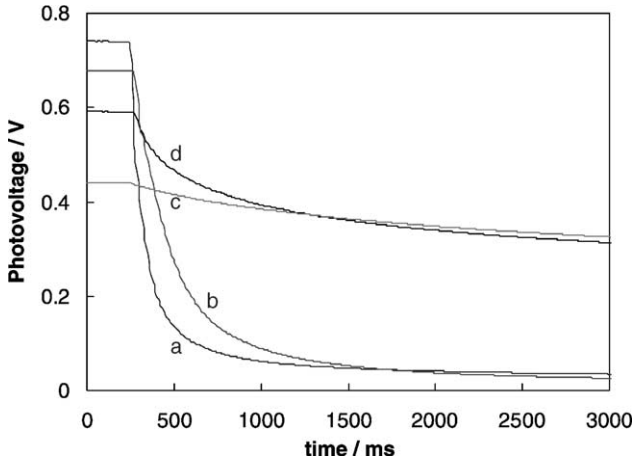

Fig. 3. Decay of the photovoltage (photovoltage, light-off transient) in DS PECs made from (a) [SnO_2]MgO (five sun), (b) [SnO_2]MgO (one sun), (c) [Sb-SnO_2]MgO (one sun) and (d) [Sb-SnO_2]MgO (five sun).

overlaps with states at the crystallite/electrolyte interface and we could write down rate of recombinations of electrons with acceptor in the electrolyte as

$$R_r = Bn_t \exp\left(-\frac{2r_c}{a}\right) \tag{2}$$

where n_t is the density of occupied traps, r_c the crystallite radius and $B = \nu_0 \exp(-E_a/kT)\Gamma$. In this expression for B, ν_0 is a characteristic frequency, E_a in the exponential term represents an activation energy and Γ is the transmission coefficient of electrons across a barrier at the crystallite/electrolyte interface. In the absence of outer shell on SnO_2, we could set $\Gamma \sim 1$ and the factor $\exp(-2r_c/a)$ in (2) makes R_r very large when $r_c \leq a$. In the presence of the barrier (i.e. MgO or ZnO shell), the transmission coefficient becomes negligibly small. The trapping rate depends on the density of unoccupied trapping sites $(N_t - n_t)$, conduction band carrier density n_e and generally written in the form

$$R_t = k_t n_e (N_t - n_t) \tag{3}$$

where $k_t = \sigma v$[25] (σ is the capture cross-section and v the thermal velocity of conduction band carriers).

Detrapping rate depends on the depth E of the trap below CBE and n_t the density of trapped electrons, i.e.

$$R_d = n_t k_d \exp\left(-\frac{E}{kT}\right) \tag{4}$$

where k_d is a characteristic "attempt to escape frequency [24]". It is most important to realize that E (depth of the trapping site below CBE) do not remain constant but depend on the electron occupation in the semiconductor and therefore on QFL. Although the system is not in equilibrium one could assume a Fermi distribution for n_e and n_t, i.e.

$$n_e = N_c \left[1 + \frac{\exp(E_c - E_f)}{kT}\right]^{-1} \tag{5}$$

$$n_t = N_t \left[1 + \frac{\exp(E_t - E_f)}{kT}\right]^{-1} \tag{6}$$

where E_c is the CBE position, E_t the position of trap level with respect to CBE and N_c the density of states in the conduction band. From (5) and (6) we get the relationship between electron occupation and the trapping energy as

$$[(N_t - n_t)n_e][(N_c - n_e)n_t]^{-1} = \exp\left(-\frac{E}{kT}\right) \tag{7}$$

where $E = E_c - E_t$. The rate equations for transport and recombinations of injected electrons into the nanocrystalline matrix can now be written in the form

$$\frac{dn_e}{dt} = G[N_c - n_e] - R_t + R_d + \frac{D_e\, d^2 n_e}{dx^2} \tag{8}$$

$$\frac{dn_t}{dt} = R_t - R_d - R_r \tag{9}$$

In Eq. (8), the rate of injection is written as $G[N_c - n_e]$ as an representation to account for the fact the rate depends on the available states. At practically realized light intensities, $n_e < N_c$. However, writing the injection rate in this form removes an singularity without affecting the behavior of the system at practically meaningful intensities of illumination. Eqs. (8) and (9), where R_t, R_d, R_r are also functions of n_e, n_t will have to be solved subject to the constraint (7). Because of the extreme nonlinearity of the system obtaining analytical solutions of these equations would be an extraordinarily difficult task. However, some useful information can be extracted as follows.

We consider the case where R_r becomes nearly independent of E, so that the recombination rate can be written in the form $R_r = k_L n_t$, where k_L is a constant (trap mediated electron leakage constant). Under steady state and open-circuit conditions (i.e. $dn_e/dt = 0$, $dn_t/dt = 0$, $dn_e/dx = 0$). The solutions of the Eqs. (7)–(9) can be expressed as

$$n_{0e} \simeq N_c - k_L k_d N_t [G(k_L + k_d + k_t N_c)]^{-1} \tag{10}$$

$$n_{0t} \simeq N_t - k_L N_t [k_L + k_d + k_t N_c]^{-1} \tag{11}$$

As the open-circuit voltage is defined by the Fermi-level up to a constant, using (11) we get the following expression for the open-circuit voltage V:

$$V \sim V_{oc} - \left(\frac{kT}{e}\right)(k_L N_t)[(k_L + k_d + k_t N_c)]^{-1} \tag{12}$$

where V_{oc} is the open-circuit voltage of the cell in the absence of trap mediated recombinations (i.e. $k_L = 0$). Eq. (12) very clearly shows how the open-circuit voltage is influenced by the trap mediated recombinations as determined by the factor $k_L N_t$. It should be noted that a higher rate of trapping (i.e. large values for N_t and or k_t) does not reduce the open-circuit voltage unless the k_L is large. This is in full agreement with our experimental results. DS SnO_2 cells yield lower voltages compared to TiO_2 because of the faster recombination rate in the former system. Outer shells of MgO or ZnO decreases k_L increasing the V_{oc}. Even more convincing are the results of our experiments with DS Sb-SnO_2 films. Here the trapping sites becomes quite high ($N_t \sim 10^{22}$) because the ionized donor (ionization energy = 0.035 meV) acts as trapping centers. For this reason V_{oc} is almost undetectable in the absence of outer shells on the Sb-SnO_2 crystallites. The short-circuit photocurrent can also expressed in asymptotic approximation as

$$I_{sc} \sim \left(\frac{D_e}{L^2}\right) \times \left[N_c - k_d k_L N_t \left(G + \frac{D_e}{L^2}\right)^{-1} (k_1 + k_d + k_t N_c)^{-1}\right] \tag{13}$$

where L is the length parameter having an order of magnitude similar to thickness of the cell and also depends on the mean free path of light in the cell. Here again trapping is seen to influence I_{sc} only if k_L is non-zero.

The expressions (10) and (11) are equilibrium solutions of the system under open-circuit conditions, transient behavior could be analyzed by setting $n_e = n_{0e} + \delta n_e$, $n_t = n_{0t} + \delta n_t$ in (10) and (11), where δn_e, δn_t denote small deviations from the equilibrium. Solution of the linearized equations with above substitution yield

$$\delta n_e = A \exp(-\Lambda_1 t) + B \exp(-\Lambda_2 t) \quad (14)$$

$$\delta n_t = C \exp(-\Lambda_1 t) + D \exp(-\Lambda_2 t) \quad (15)$$

The time constants Λ_1, Λ_2 given by

$$\Lambda_1 = \left(N_c - \frac{k_L N_t}{G} \right) k_t + k_L,$$

$$\Lambda_2 = G - k_t^2 N_t N_c [k_L + k_d + k_t N_c] \quad (16)$$

dictates the transient voltage responses (note: $\delta V \sim \delta n_e / n_{0e}$). It is interesting to note that the first time constant is quite sensitive to trap mediated recombinations, whereas the second depends weakly on k_L. This shows that in the transients (unlike in the equilibrium situation), the effect of trapping becomes detectable, even if the trap mediated electron leakage is negligible. Fig. 1 shows the photovoltage, light-on transients of DS cells made from SnO_2, [SnO_2]MgO and [Sb-SnO_2]MgO films. The respective time constants ($\sim[\Lambda_1 + \Lambda_2]^{-1}$) are ~7, 3, 40 s, respectively, showing the effects on trapping and electron leakage. Photocurrent transients show similar behavior with two time constants which depends on D_e in addition to other constants in (16). An improvement of the sharpness of the photocurrent transients of [SnO_2]MgO system compared to SnO_2 clearly seen (Fig. 2). Fig. 2 also shows the photocurrent transients for DS TiO_2 cell under same conditions. We believe that the slowness of the response here (compared to [SnO_2]MgO) originates from smaller diffusion coefficient of electron transport in TiO_2, because of the larger electron effective mass in TiO_2. The gross features of the transients we have obtained agrees with above predictions. The intensity dependence of time constants (i.e. originating from Λ_2) is noticeable in DS [SnO_2]MgO (Fig. 3). Another interesting effect we observed was, how the photocurrent transients of [SnO_2]MgO changes as thickness of the MgO shell is increased. At the shell thickness which gives the optimum efficiency for the DS [SnO_2]MgO cell, the response become faster than that of DS SnO_2 and as the shell thickness is further increased the response gets progressively slower. When the MgO shell thickness becomes larger, direct tunneling of electron (released by the excited dye molecule on MgO surface) through the shell is unlikely. The electron first enters a trap level in MgO and then passes to the conduction band of SnO_2, the delay associated with trap mediation is reminiscent in the transients. Further experimentation would be necessary to determine time constants separately and under different conditions.

In the above analysis we assumed that conduction band electron states do not get directly involved in recombinations with the acceptors in the electrolyte. The reason is that conduction band electrons are well screened from electrolyte owing to depletion. We found that both in quantum mechanical and classical regimes strong confinement become possible and the extent of confinement is determined by parameters such as effective electron mass, dielectric constant and donor density.

The solid-state DS solar cell in principle is a more neat system with out the complications of a liquid electrolyte [25–31]. However, the recombination problems seem to be more severe in the solid-state system. The best reported efficiency is ~4% for cell which uses CuI as the hole collector [29,32,33]. Undoubtedly, even in this case the trap mediated recombinations plays a dominant role. A simpler way to look at recombinations in the DS solid-state cell would be to adopt Shockley–Read formalism, because in this case both electrons and holes are involved. If for simplicity, we assume that one single interface trap captures electrons and holes with cross-sections S_n and S_p, respectively. The Shockley–Read [34,35] formula for the recombination rate (P) then takes the simple form

$$P = S_n S_p N_i q v [S_n + S_p]^{-1} \quad (17)$$

where N_i is the interface trap density, q the electron density = hole density and v is a surface recombination velocity. Thus reduction in one capture cross-section (i.e. S_n or S_p) will curtail recombinations to a great extent. There is some evidence to support the importance of this effect. We found that solid-state DS solar cells made from nanocrystalline films of SnO_2 gives no measurable photovoltaic response. However, once the crystallite surface is deposited with a ultra-thin shell (e.g. Al_2O_3 or ZnO) cells get activated [36,37]. Presumably as a result of the delocalization of trapped electrons in SnO_2 as explained earlier, the capture of electrons by interface defects becomes the rate determining step. A the barrier on SnO_2 greatly reduces the capture cross-section of electrons. Although, ultra-thin shells of insulating or high band gap semiconducting materials on crystallites do not show an improvement in the wet TiO_2-based DS cells, we have noted that insulating shells on the crystallites do improve the solid-state version. This shows that the interface in the solid-state cells is more susceptible to capture of electrons.

4. Conclusion

The main motivation for construction of the above theoretical model is the insight we gained by experimentation with DS photoelectrochemical and solid-state solar cells made from SnO_2, Sb-SnO_2, ZnO and composite crystallite systems. This study enabled us understand intrinsic difference between TiO_2 and two most familiar oxide semiconducting materials, i.e. SnO_2 and ZnO used for dye-sensitization experiments. Out come of the investigation was that the recombinations of electrons injected to the semiconductor with acceptors depend on the extent of spread of the wave function of electrons trapped in shallow levels. The complication

in mathematical analysis comes from the dependence of the rate constants on the QFL which vary with the electron occupation. We could not solve the equations to define the *I–V* characteristics and tell how the efficiency would respond to the extent of trapping. We believe that intensity modulated photocurrent and photovoltage spectroscopic measurements on system we have examined would assist further elucidation of the mechanisms involved. Recombinations via conduction band states cannot be completely neglected. Further investigations seems to be necessary to determine how the conduction band electrons interact directly with the interface. We have no information as to how the ultra-thin shells on the crystallites affects the charge injection rate. The indication is that the rate is not much decreased by an ultra-thin barrier, as the energy of the electron released with de-excitation of the dye molecule is well above the CBE. Further understanding of this problem require time resolved measurements.

References

[1] M. Gratzel, Nature 414 (2001) 338.
[2] D. Cahen, M. Gratzel, J.F. Guillemoles, G. Hodes, in: G. Hodes (Ed.), Electrochemistry of Nanomaterials, Wiley/VCH, Weinheim, 2000, pp. 201–227.
[3] T. Hannappel, B. Burfeindt, W. Storck, F. Willig, J. Phys. Chem. 101 (1997) 6799.
[4] J.M. Rehm, G.L. Mclendon, Y. Nagasawa, K. Yoshihara, J. Moser, M. Gratzel, J. Phys. Chem. 100 (1996) 9577.
[5] J.B. Asbury, H.N. Gosh, J.R. Ellingson, S. Ferrere, A.J. Nozik, T. Lain, Femtosecond IR study of Ru dye sensitized nanocrystalline TiO_2 thin films: ultrafast electron injection and relaxation dynamics, Ultrafast Phenomenon XI, 1998.
[6] S. Yan, J.T. Hupp, J. Phys. Chem. 100 (1996) 6867.
[7] I. Martini, J.H. Hodak, G.V.J. Hartland, J. Phys. Chem. B 102 (1998) 607.
[8] M. Hilgendroff, V. Sundstrom, J. Phys. Chem. 14 (2002) 190.
[9] S. Sodergren, A. Hagfeldt, J. Olsson, S.E. Lindquist, J. Phys. Chem. 98 (1994) 5552.
[10] A. Solbrand, S. Sodergren, H. Lindstrom, H. Rensmo, A. Hagfeldt, S.E. Lindquist, J. Phys. Chem. B 101 (1997) 2514.
[11] L.M. Peter, D. Vanmaekelbergh, in: R.C. Alkire, D.M. Kolb (Eds.), Advances in Electrochemical Sciences and Engineering, vol. 6, Wiley/Interscience, New York, 1999, p. 77.
[12] P.E. de Jongh, D. Vanmaekelbergh, Phys. Rev. Lett. 77 (1996) 3427.
[13] K. Schwarzburg, F. Willig, Appl. Phys. Lett. 58 (1991) 2520.
[14] R. Konenkamp, R. Hennniger, P. Hoyer, J. Phys. 97 (1993) 7328.
[15] P. Hoyer, R. Eichberger, H. Weller, Ber. Bunsen-Ges. Phys. Chem. 97 (1993) 630.
[16] J. Nelson, Phys. Rev. B 59 (1999) 15374.
[17] K. Tennakone, J. Bandara, P.K.M. Bandaranayake, G.R.R.A. Kumara, A. Konno, Jpn. J. Appl. Phys. 40 (2001) L732.
[18] K. Tennakone, P.K.M. Bandaranayake, P.V.V. Jayaweera, A. Konno, G.R.R.A. Kumara, Physica E, in press.
[19] K. Tennakone, P.K.M. Bandaranayake, P.V.V. Jayaweera, J. Bandara, A. Konno, G.R.R.A. Kumara, S. Kaneko, in: Proceedings of the 200th International Meeting of the Electrochemical Society, Abstract 1079, 2001.
[20] K. Tennakone, G.R.R.A. Kumara, I.R.M. Kottegoda, V.P.S. Perera, J. Chem. Soc., Chem. Commun. (1999) 15.
[21] K. Tennakone, I.R.M. Kottegoda, L.L.A. De Silva, V.P.S. Perera, Semicond. Sci. Technol. 14 (1999) 975.
[22] A.S. Branski, W.R. Fawcett, J. Electrochem. Soc. 127 (1980) 1766.
[23] R.P. Feyman, R.B. Leighton, M. Sands, Lectures on Physics, vol. 3, Narosa Publishing House, New Delhi, 1997, pp. 1641–1643.
[24] R.H. Bube, Photoelectronic Properties of Semiconductors, Cambridge University Press, Cambridge, 1992, pp. 1–3.
[25] K. Tennakone, K.P. Hewaparakkrama, M. Devasurendra, A.H. Jayatissa, L.K. Weerasena, Semicond. Sci. Technol. 3 (1988) 382.
[26] K. Tennakone, G.R.R.A. Kumara, A.R. Kumarasinghe, K.G.U. Wijayantha, P.M. Srimanne, Semicond. Sci. Technol. 10 (1995) 1689.
[27] B.O. Regan, D.T. Schwartz, Chem. Mater. 7 (1995) 1349.
[28] B.O. Regan, D.T. Schwartz, J. Appl. Phys. 80 (1996) 4749.
[29] K. Tennakone, G.R.R.A. Kumara, I.R.M. Kottegoda, K.G.U. Wijayantha, V.P.S. Perera, J. Phys. D 31 (1998) 1492.
[30] U. Bach, D. Lupo, P. Comte, J.E. Moser, F. Weissortel, J. Salbeck, H. Spretezer, M. Gratzel, Nature 395 (1998) 583.
[31] K. Tennakone, G.K.R. Senadeera, D.B.R. De Silva, I.R.M. Kottegoda, Appl. Phys. Lett. 77 (2000) 2367.
[32] G.R.R.A. Kumara, A. Konno, K. Shiratsuchi, J. Tsukahara, K. Tennakone, Chem. Mater. 14 (2002) 954.
[33] Q.B. Meng, X.T. Zhang, C.H. Fu, Z.C. He, O.A. Semenikhin, O. Sato, T.N. Rao, L. Sutanto, M. Okuyama, A. Fujishima, H. Watanabe, M. Uragami, in: Proceedings of the International Workshop on Photochemistry, Abstracts, Tokyo, January 2002, p. 9.
[34] W. Shockley, W.T. Read, Phys. Rev. 87 (1952) 835.
[35] S.M. Sze, Physics of Semiconductor Devices, 2nd ed., Wiley/Interscience, New York, 1981, pp. 35–38.
[36] K. Tennakone, V.P.S. Perera, I.R.M. Kottegoda, L.A.A. De Silva, G.R.R.A. Kumara, A. Konno, J. Electron. Mater. 30 (2001) 992.
[37] K. Tennakone, V.P.S. Perera, I.R.M. Kottegoda, G.R.R.A. Kumara, J. Phys. D 32 (1999) 374.